Magnetic Field, Force, and Inductance Computations for an Axially Symmetric Solenoid

John E. Lane
Dynacs, Inc., Kennedy Space Center, Florida

Robert C. Youngquist
NASA, Kennedy Space Center, Florida

Christopher D. Immer
Dynacs, Inc., Kennedy Space Center, Florida

James C. Simpson
NASA, Kennedy Space Center, Florida

April 2001

Since its founding, NASA has been dedicated to the advancement of aeronautics and space science. The NASA Scientific and Technical Information (STI) program plays a key part in helping NASA maintain this important role.

The NASA STI Program operates under the auspices of the Agency Chief Information Officer. It collects, organizes, provides for archiving, and disseminates NASA's STI. The NASA STI program provides access to the NASA Aeronautics and Space Database and its public interface, the NASA Technical Reports Server, thus providing one of the largest collections of aeronautical and space science STI in the world. Results are published in both non-NASA channels and by NASA in the NASA STI Report Series, which includes the following report types:

- TECHNICAL PUBLICATION. Reports of completed research or a major significant phase of research that present the results of NASA programs and include extensive data or theoretical analysis. Includes compilations of significant scientific and technical data and information deemed to be of continuing reference value. NASA counterpart of peer-reviewed formal professional papers but has less stringent limitations on manuscript length and extent of graphic presentations.

- TECHNICAL MEMORANDUM. Scientific and technical findings that are preliminary or of specialized interest, e.g., quick release reports, working papers, and bibliographies that contain minimal annotation. Does not contain extensive analysis.

- CONTRACTOR REPORT. Scientific and technical findings by NASA-sponsored contractors and grantees.

- CONFERENCE PUBLICATION. Collected papers from scientific and technical conferences, symposia, seminars, or other meetings sponsored or cosponsored by NASA.

- SPECIAL PUBLICATIONS. Scientific, technical, or historical information from NASA programs, projects, and missions, often concerned with subjects having substantial public interest.

- TECHNICAL TRANSLATION. English-language translations of foreign scientific and technical material pertinent to NASA's mission.

Specialized services also include creating custom thesauri, building customized databases, organizing and publishing research results.

For more information about the NASA STI program, see the following:

- Access the NASA STI program home page at http://www.sti.nasa.gov

- E-mail your question via the Internet to help@sti.nasa.gov

- Fax your question to the NASA STI Help Desk at 443-757-5803

- Telephone the NASA STI Help Desk at 443-757-5802

- Write to:
  NASA Center for Aerospace Information (CASI)
  7115 Standard Drive
  Hanover, MD 21076-1320

NASA/TM—2013–217918

Magnetic Field, Force, and Inductance Computations for an Axially Symmetric Solenoid

John E. Lane
Dynacs, Inc., Kennedy Space Center, Florida

Robert C. Youngquist
NASA, Kennedy Space Center, Florida

Christopher D. Immer
Dynacs, Inc., Kennedy Space Center, Florida

James C. Simpson
NASA, Kennedy Space Center, Florida

April 2001

NASA/TM—2013–217918

Preface

In the late 1990s research was being performed at the Kennedy Space Center to develop *in situ* resource utilization technology for Mars. One study topic was the generation and storage of liquid oxygen (LOX) obtained from the atmosphere or regolith, but the transfer of this commodity was of concern. Mechanical LOX pumps were deemed potentially too heavy and unreliable for an autonomous mission to Mars, and alternatives were sought. One option was to use the paramagnetic property of LOX, which is significant enough that small quantities of LOX can be suspended against earth gravity with a rare earth magnet. With this application in mind, a small, internally funded project was initiated at the Kennedy Space Center in 2000 to study the use of pulsed magnetic fields to pump LOX.

Proof-of-concept testing verified the LOX pumping predictions and resulted in a journal publication [1]. Numerous small coils were fabricated on cryogenic flow lines and used to produce intense, short-duration magnetic fields resulting in dramatic motion of the LOX. In addition, effort was expended on modeling the paramagnetic forces in the LOX, which required modeling the magnetic field generated by the coils and the coil inductance, allowing the current versus time to be predicted and compared to experiment.

During the coil inductance modeling, we generated a method by which the inductance of an air-core solenoid could be computed efficiently. We wrote a short manuscript documenting this work, but did not proceed with publication. Instead, we chose to release our software (primarily generated by one of the authors, John Lane) with the manuscript attached as a reference document. The software and manuscript were made public through the Open Channel Foundation, an organization that publishes software from academic and research institutions. The link for this site is given below.

http://www.openchannelfoundation.org/project/view_docs.php?group_id=288

Through this link, our manuscript has been downloaded multiple times, has been used by several researchers, but to our knowledge, has not been cited. We suspect that this may be due to the lack of a clear citation and have decided that one should be provided. We consider it too late to seek peer-reviewed publication of this work and instead have decided to issue a NASA Technical Memorandum, with the same title and authors as the original manuscript. This will allow our work to be located by the search engines and will provide a reliable, long-term source and citation. The original manuscript, reformatted, but not in any other way altered, appears on the subsequent pages of this memorandum.

[1]   Youngquist, Robert C., Immer, Christopher D., Lane, John E., and Simpson, James C., "Dynamics of a Finite Liquid Oxygen Column in a Pulsed Magnetic Field," *IEEE Transactions on Magnetics,* **39**(4), July 4, 2003, pp. 2068–2073.

This page was intentionally left blank.

Contents

Figures

Tables

This page was intentionally left blank.

1 INTRODUCTION

The pumping of liquid oxygen (LOX) by magnetic fields (B field), using an array of electromagnets, is a current topic of research and development at Kennedy Space Center, FL. Oxygen is paramagnetic so that LOX, like a ferrofluid, can be forced in the direction of a B field gradient. It is well known that liquid oxygen has a sufficient magnetic susceptibility that a strong magnetic gradient can lift it in the earth's gravitational field. It has been proposed that this phenomenon can be utilized in transporting (i.e., pumping) LOX not only on earth, but on Mars and in the weightlessness of space.

In order to design and evaluate such a magnetic pumping system, it is essential to compute the magnetic and force fields, as well as inductance, of various types of electromagnets (solenoids). In this application, it is assumed that the solenoids are air wrapped, and that the current is essentially time independent.

2 B FIELD EVALUATION

The magnetic field **B** due to a single current loop of radius a, as shown in Figure 1, can be computed by evaluating the curl of the magnetic *vector potential* **A**. With the current loop located in and symmetric with respect to the x-y plane, **A** is given by [1]:

$$A_\varphi(r,\theta) = \frac{\mu_0 a I}{4\pi} \int_0^{2\pi} \frac{\cos\varphi'\, d\varphi'}{\sqrt{a^2 + r^2 - 2ar\sin\theta\cos\varphi'}} \tag{1}$$

where r, θ, and ϕ' are spherical coordinates, i is the loop current, and μ_0 is the *permeability* of free space. The curl of Equation (1) can be simplified in cylindrical coordinates [2], or in Cartesian coordinates as follows [3]:

$$B_x(x,y,z) = \frac{C\,x\,z}{2\alpha^2\beta\rho^2}\left((a^2+R^2)E(k^2) - \alpha^2 K(k^2)\right) \tag{2a}$$

$$B_y(x,y,z) = \frac{C\,y\,z}{2\alpha^2\beta\rho^2}\left((a^2+R^2)E(k^2) - \alpha^2 K(k^2)\right) \tag{2b}$$

$$B_z(x,y,z) = \frac{C}{2\alpha^2\beta}\left((a^2-R^2)E(k^2) + \alpha^2 K(k^2)\right) \tag{2c}$$

where $\rho^2 \equiv x^2 + y^2$, $R^2 \equiv \rho^2 + z^2$, $\alpha^2 \equiv a^2 + R^2 - 2a\rho$, $\beta^2 \equiv a^2 + R^2 + 2a\rho$, $k^2 \equiv 1 - \alpha^2/\beta^2$, and $C \equiv \mu_0\, i/\pi$. $E(k^2)$ and $K(k^2)$ are the complete elliptic integrals of the first and second kind, respectively.
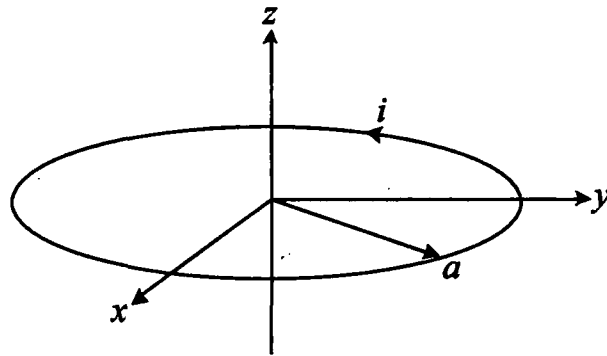
Figure 1. Circular current loop.

3 FORCE FIELD EVALUATION

In order to estimate the force on a paramagnetic volume of LOX, it is necessary to evaluate the force equation [4]:

$$F = \frac{1}{\mu_0}\left(\frac{\chi}{1+\chi}\right)(B \cdot \nabla)\, B \qquad (3)$$

where again μ_0 is the *permeability* of free space and χ is the *magnetic susceptibility* of the medium. Equation (3) can be rewritten in matrix form as:

$$F = \frac{1}{\mu_0}\left(\frac{\chi}{1+\chi}\right) D\, B \qquad (4)$$

where

$$D \equiv \begin{pmatrix} \dfrac{\partial B_x}{\partial x} & \dfrac{\partial B_x}{\partial y} & \dfrac{\partial B_x}{\partial z} \\[2mm] \dfrac{\partial B_y}{\partial x} & \dfrac{\partial B_y}{\partial y} & \dfrac{\partial B_y}{\partial z} \\[2mm] \dfrac{\partial B_z}{\partial x} & \dfrac{\partial B_z}{\partial y} & \dfrac{\partial B_z}{\partial z} \end{pmatrix} \qquad (5)$$

It can be shown that D can be written as:

$$D = P\,E\left(k^2\right) + Q\,\alpha^2\, K\left(k^2\right) \qquad (6)$$

$$P = \begin{pmatrix} p_1 & p_2 & p_3 \\ p_2 & p_4 & \frac{y}{x}p_3 \\ p_3 & \frac{y}{x}p_3 & p_5 \end{pmatrix} \qquad Q = \begin{pmatrix} q_1 & q_2 & q_3 \\ q_2 & q_4 & \frac{y}{x}q_3 \\ q_3 & \frac{y}{x}q_3 & q_5 \end{pmatrix} \qquad (7)$$

where $\mathbf{P}$ and $\mathbf{Q}$ are symmetric matrices. The five independent components of $\mathbf{P}$ and $\mathbf{Q}$ are given in Appendix A and Appendix B, in terms of the x, y, z field coordinates and loop radius a, where $\gamma^2 \equiv x^2 - y^2$ [3].

4 INDUCTANCE FORMULAS

A common method of computing inductance of a solenoid in many engineering applications is to identify a handbook formula that most closely resembles the particular solenoid geometry at hand. Afterwards, a fine-tuning can be performed when building the coil by adding or subtracting loops of wire.

For example, an estimate of the total inductance L of a single circular current loop is given by:

$$L = a\mu_0 \left[\ln(8a/b) - \tfrac{7}{4} \right] \tag{8}$$

where a is the loop radius and b the wire cross-sectional radius, as shown in Figure 2. This estimate of self-inductance is good as long as $b/a \ll 1$.
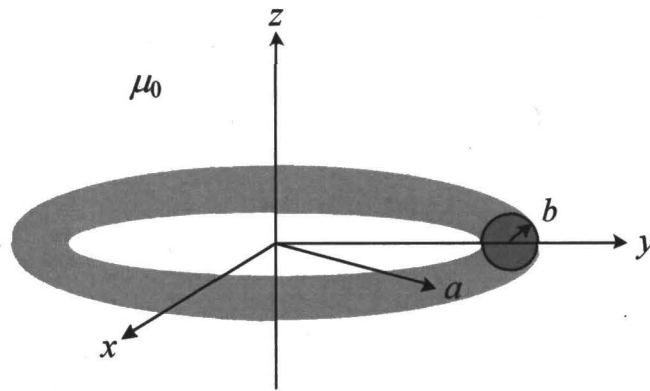

Figure 2. Circular current loop of radius a with finite cross-sectional radius b.

4.1 Stacked Single Layer

Figure 3 diagrams a stack of M current loops, as would be found in a single layered solenoid. The handbook formula [5] for approximating inductance of this configuration is:

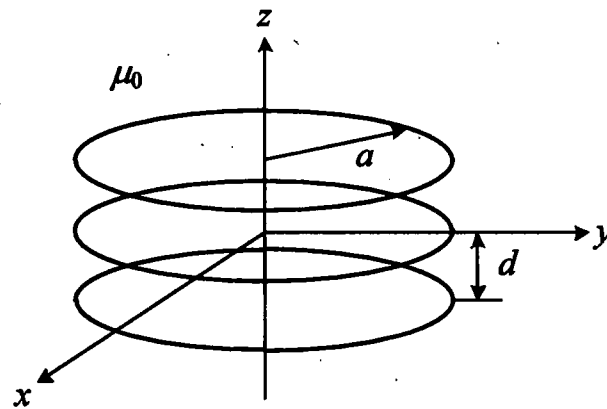$$L = \frac{\pi\mu_0 a^2 M^2}{\sqrt{4a^2 + (M-1)^2 d^2}} \tag{9}$$

Figure 3. *M* stacked current loops.

4.2   Stacked Multiple Layers

Figure 4 depicts a stack of M_z current loops, configured as M_x layers, as would be found in a multi-layered solenoid. The handbook formula [6] for approximating inductance of this configuration is:

$$L = \frac{\pi \mu_0 \, r_0^3 (M_x M_z)^2}{r_0 l + 0.9 \, r_0^2 + 0.32 \, l \, t + 0.84 r_0 t} \tag{10a}$$

$$l \equiv (M_z - 1) \, d_z \quad t \equiv 2 M_x b$$
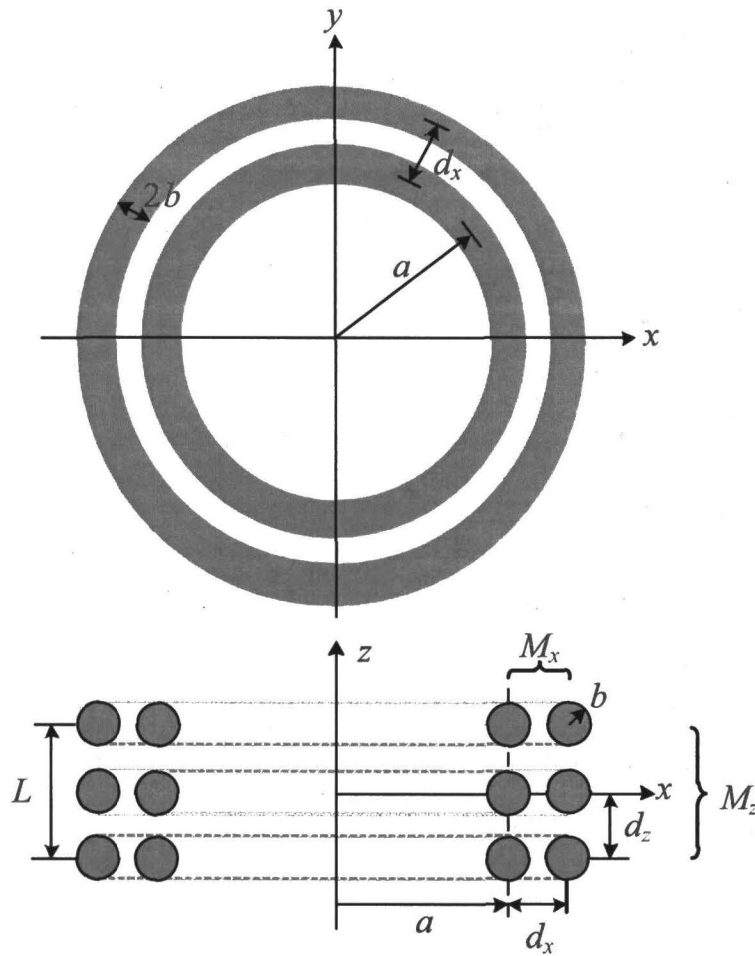$$r_0 \equiv a + (M_x - 1) \, b \tag{10b}$$

Figure 4. Stacked multiple layer coil.

4.3   Inductance From the Stored Energy

Inductance L can be derived from the energy stored in a magnetic field due to a current carrying wire. In this case, L is equal to the integral of the product of current density **J** and magnetic vector potential **A**, divided by current squared [1]:

$$L = \frac{1}{i^2} \int \mathbf{J} \cdot \mathbf{A} \; dx^3 \tag{11}$$

For a single wire loop of wire diameter b and loop diameter a, the magnetic vector potential inside the wire can be approximated by [1]:

$$\mathbf{A} = \frac{\mu_0 i}{4\pi} \left[\left(1 - \frac{\rho^2}{b^2} \right) + 2 \left(\ln \frac{8a}{b} - 2 \right) \right] \hat{\mathbf{e}}_\varphi \tag{12}$$

with the assumption that $b/a \ll 1$. Assuming also that the current density is uniform (no high frequency skin effects, etc.), then $\mathbf{J} = i / \pi b^2 \; \hat{\mathbf{e}}_\varphi$. Integrating $\mathbf{J} \cdot \mathbf{A}$ over the wire cross-section and

total length, as described by Equation (11), and dividing by i^2 leads to an approximation of self-inductance given by Equation (8). Note that due to symmetry, the volume integral becomes a line integral, $\int dx^3 \rightarrow 4\pi^2 a \int_0^b \rho\, d\rho$.

Equation (8) describes an approximation to the total inductance of a single circular wire loop, which becomes exact as b/a approaches zero. When multiple loops are considered, as would be found in a solenoid, the total inductance is the sum of two parts, *self-inductance* and *mutual-inductance*. Using Figure 4 as a general solenoid model, composed of M_z stacks and M_x layers, such that the total number of loops is equal to $M_x M_z$.

The total solenoid inductance can be computed by summing the self-inductance and mutual inductance contributions of each mth, n^{th} loop (refer to Figure 5):

$$L = \sum_{m=-(M_z-1)/2}^{(M_z-1)/2} \sum_{n=0}^{M_x-1} \left(L_{mn} + M_{mn} \right) \tag{13}$$

where the self-inductance of the mth, n^{th} loop is approximated by Equation (1):

$$L_{mn} = \mu_0 a_n \left[\ln\left(8a_n/b\right) - \tfrac{7}{4} \right] \tag{14}$$

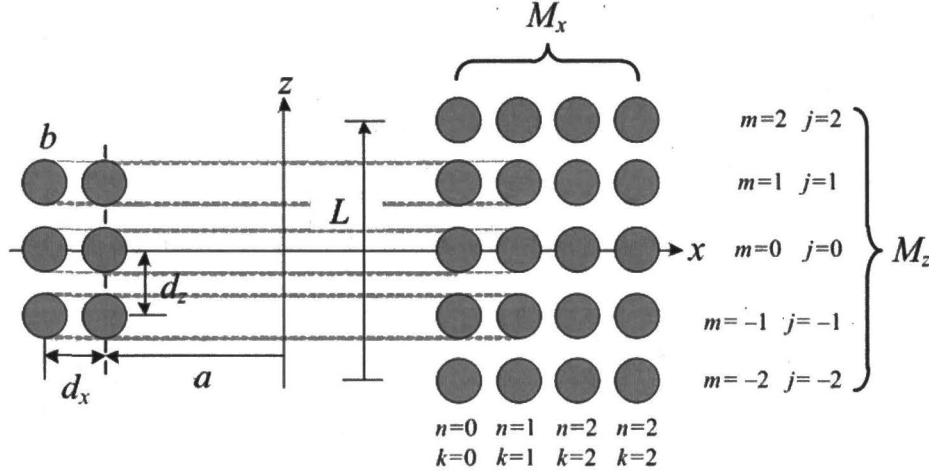where a is replaced with $a_n = a + nd_x$.

Figure 5. Solenoid model for general inductance calculation.

The mutual inductance component M_{mn} of each wire loop is determined by considering the magnetic vector potential of a single loop centered at the origin, in spherical coordinates:

$$\mathbf{A} = \frac{\mu_0 i a}{\pi\sqrt{a^2 + r^2 + 2ar\sin\theta}} \left[\frac{(2-\phi)K(\phi) - 2E(\phi)}{\phi} \right] \hat{\mathbf{e}}_\varphi \tag{15a}$$

$$\phi = \frac{4ar\sin\theta}{a^2 + r^2 + 2ar\sin\theta} \tag{15b}$$

where $K(\varphi)$ and $E(\varphi)$ are again the complete elliptic integrals of the first and second kind, respectively.

Equations (15) can be used to describe the magnetic vector potential from each mth, n^{th} wire loop, simply by translating the coordinate system. The r coordinate in Equations (15) describes the field at the mth, n^{th} wire loop due to the jth, k^{th} wire loop, excluding the self-potential where $j = m$ and $k = n$. To quantify this relationship, it can be shown that by following definitions given Figure 5, r in Equations (15) becomes:

$$r_{jkmn} = \sqrt{a_n^2 + (m-j)^2 d_z^2} \tag{16a}$$

leading to the associated modification of Equation (15b):

$$\varphi_{jkmn} = \frac{4 a_k a_n}{(a_k + a_n)^2 + (m-j)^2 d_z^2} \tag{16b}$$

where $a_k = a + k d_x$. The magnetic vector potential from Equation (8a) for each mth, n^{th} wire loop now becomes:

$$(A_\varphi)_{jkmn} = \left(\frac{\mu_0 i \sqrt{(a_k + a_n)^2 + (m-j)^2 d_z^2}}{\pi \, a_n} \right) \cdot \left((2 - \phi_{jkmn}) K(\phi_{jkmn}) - 2E(\phi_{jkmn}) \right) \tag{17}$$

Finally, to express the mutual inductance of the mth, n^{th} wire loop, the integral of Equation (11) can be approximated by a simple product of the wire cross-section with a summation of Equation (17) over j and k, excluding $j = m$ and $k = n$:

$$M_{mn} = \frac{\mu_0}{2} \sum_{\substack{j=-(M_z-1)/2 \\ (\text{excluding } j=m,\, k=n)}}^{(M_z-1)/2} \sum_{k=0}^{M_x-1} \sqrt{(a_k + a_n)^2 + (m-j)^2 d_z^2} \cdot \left\{ (2 - k_{mnjk}^2) K(k_{mnjk}^2) - 2E(k_{mnjk}^2) \right\} \tag{18}$$

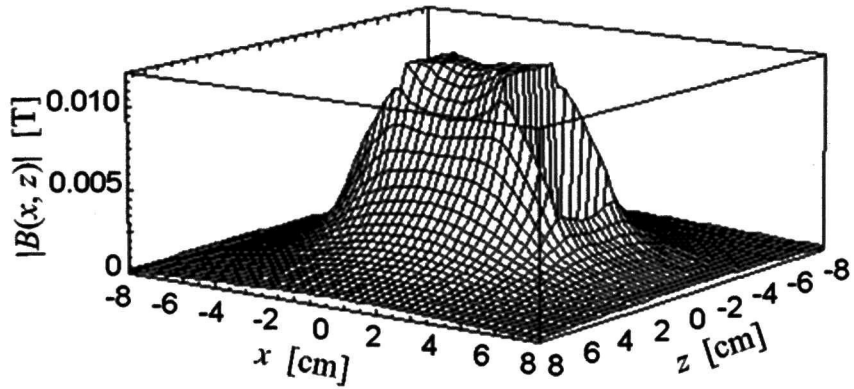## 5   EXPERIMENTAL RESULTS AND DISCUSSION

Magnetic field and force plots using two example coils are generated by employing Equations (2) and (4). The first coil has dimensions of $a = 20$ mm, $b = 0.5$ mm, $d_x = d_z = 1$ mm, $M_x = 20$, and $M_z = 31$. The B and force field plots are shown in Figures 6a and 6b. Figures 6c and 6d are the B and force field plots of coil #7 in Table 1.
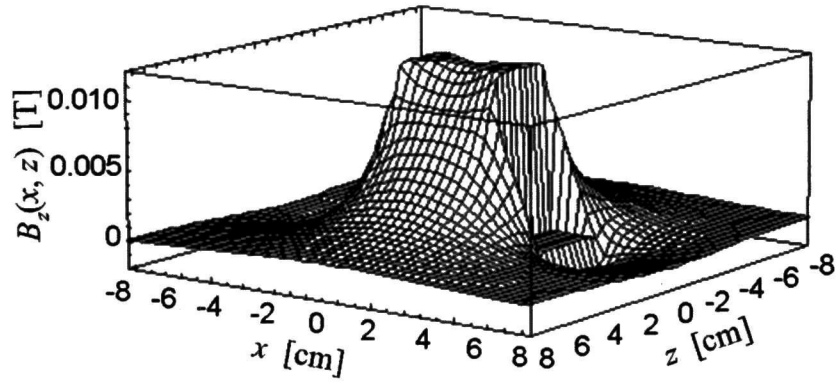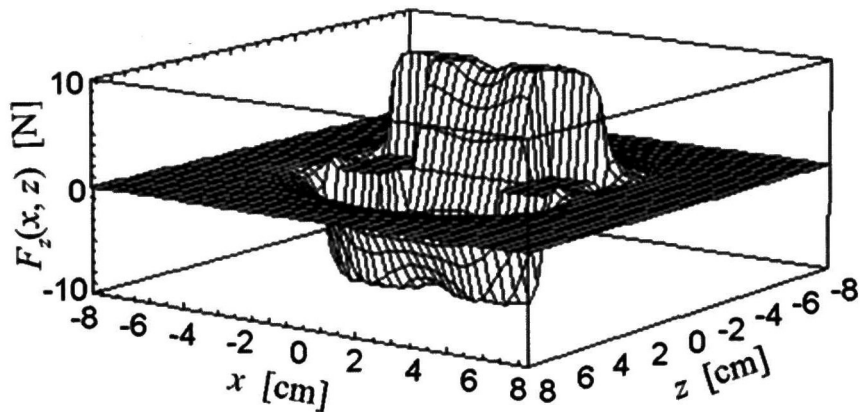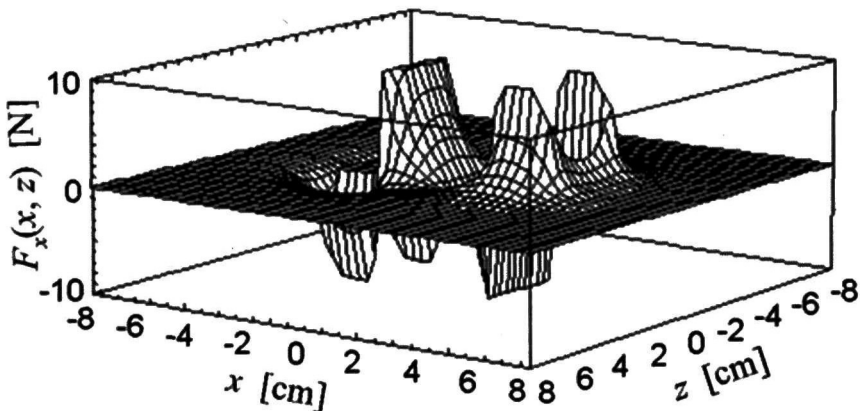
$B_z(x,0,z)$
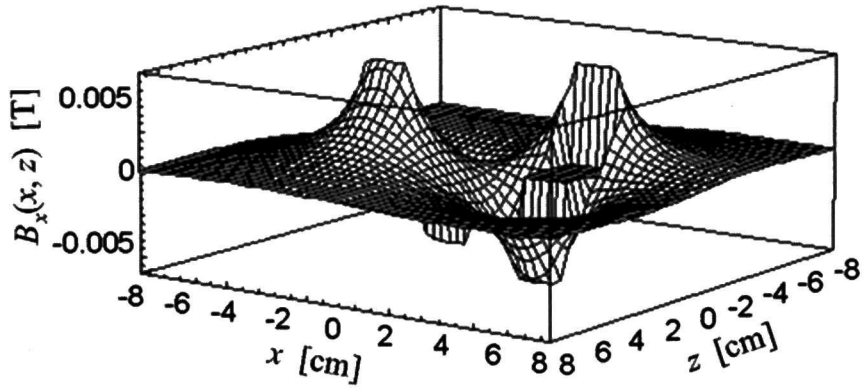
$B_x(x,0,z)$

$|B(x,0,z)|$

Figure 6a. Solenoid B-field plots from Equations (2) with dimensions $a = 20$ mm, $b = 0.5$ mm, $d_x = d_z = 1$ mm, $M_x = 20$, and $M_z = 31$.
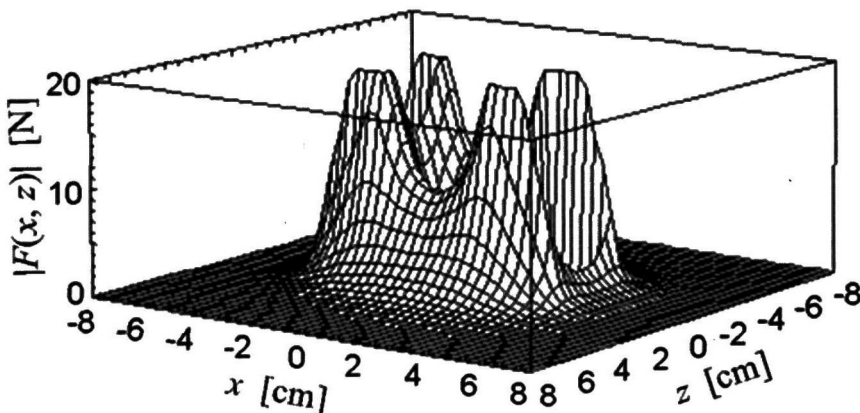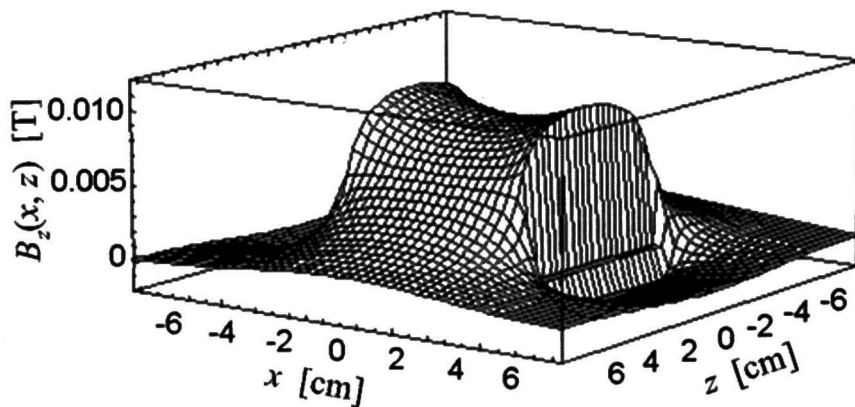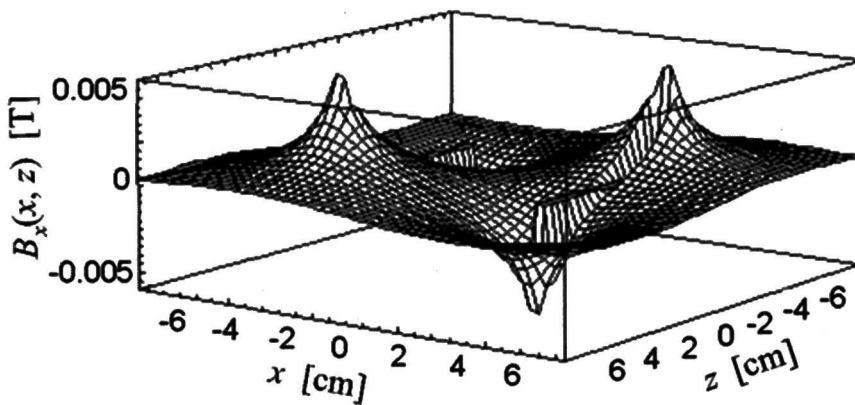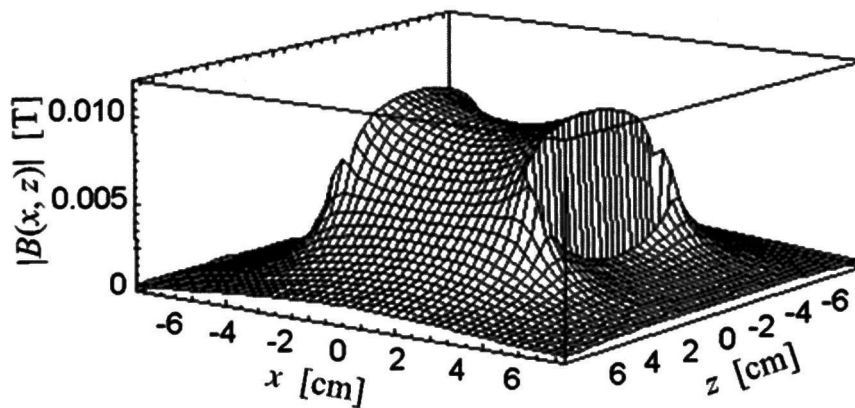
$F_z(x,0,z)$

$F_x(x,0,z)$

$|F(x,0,z)|$

Figure 6b. Solenoid F-field plots from Equation (4) with dimensions $a = 20$ mm, $b = 0.5$ mm, $d_x = d_z = 1$ mm, $M_x = 20$, and $M_z = 31$.

$B_z(x,0,z)$

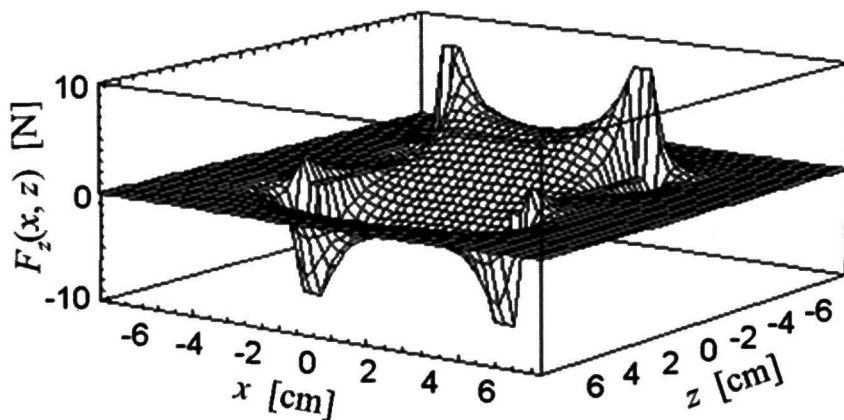$B_x(x,0,z)$
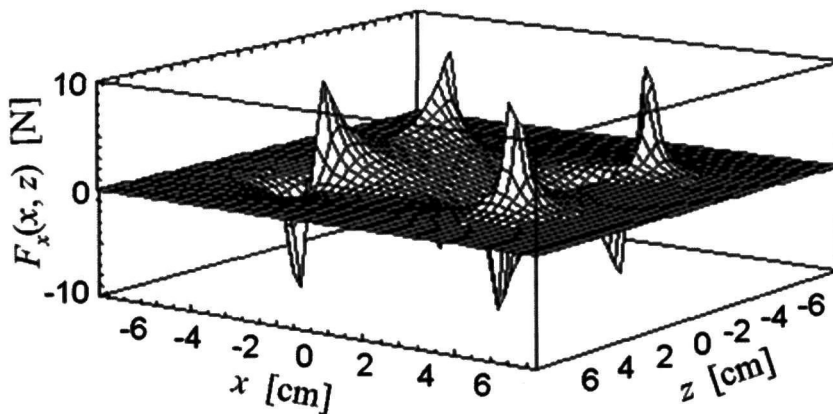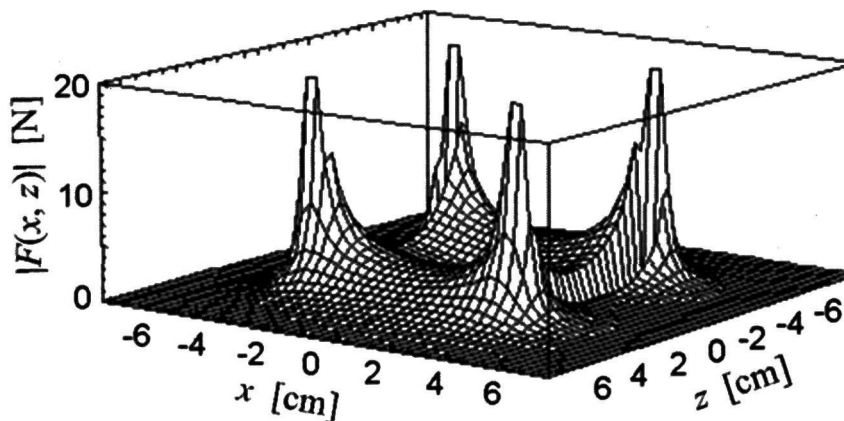
$|B(x,0,z)|$

Figure 6c. Solenoid B-field plots from Equations (2) with dimensions
$a = 32.1$ mm, $b = 0.362$ mm, $d_x = 0.683$, $d_z = 0.757$ mm, $M_x = 8$, and $M_z = 83$.

$F_z(x,0,z)$

$F_x(x,0,z)$

$|F(x,0,z)|$

Figure 6d. Solenoid F-field plots from Equation (4) with dimensions
a = 32.1 mm, b = 0.362 mm, d_x = 0.683, d_z = 0.757 mm, M_x = 8, and M_z = 83.

Table 1. Dimensions of test coils [mm].

Coil #	a	b	d_x	d_z	M_x	M_z
1	6.41	0.051	0.011	0.013	4	150
2	4.57	0.127	0.240	0.277	27	11
3	4.70	0.255	0.470	0.540	21	33
4	4.70	0.255	0.540	0.540	27	15
5	4.60	0.140	0.267	0.280	31	19
6	1.67	0.080	0.170	0.178	17	19
7	32.1	0.362	0.683	0.757	8	83/84

Equations (13), (14), and (18) make up a complete description of the total inductance of a solenoid described by Figure 5. In order to get some qualitative insight into the relative accuracy of this description of inductance, it is helpful to plot the self-inductance and mutual-inductance contributions, as shown in Figures 7 and 8. For these particular examples, the mutual inductance contribution quickly dominates as the number of turns increases. This implies that error resulting from the simplifying assumption of $b/a \ll 1$, used to compute the self-inductance term in Equation (14), will in most cases not be the primary source of error. Therefore, it can be concluded that accuracy of this method for computing solenoid inductance is dominated by the error introduced by allowing the integral in Equation (11) to be calculated as a product of the magnetic potential at the center of the wire cross-section times the cross-sectional area.
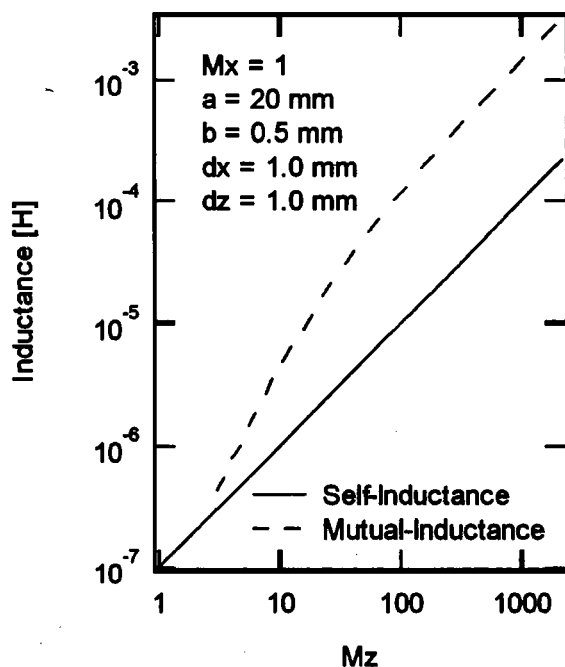

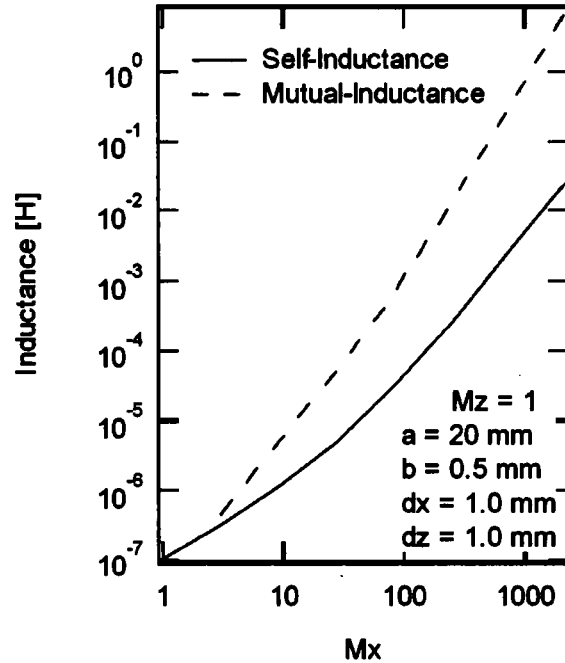Figure 7. Self- and mutual-inductance vs. M_z for $M_x = 1$.

Figure 8. Self- and mutual-inductance vs. M_x for $M_z = 1$.

Figure 9 compares the calculated to the measured inductance of seven coils with dimensions given in Table 1. "L Model #2" is equivalent to Equation (9); "L Model #3" is described by Equations (10); and "L Model #4" is represented by Equations (13), (14), and (18). Note that the simple approximation from L Model #3 seems to consistently track the more accurate calculation of L Model #4. Figure 10 is similar to Figure 9, but was generated using a Monte Carlo approach, comparing all inductance formula calculations to Model #4 results.
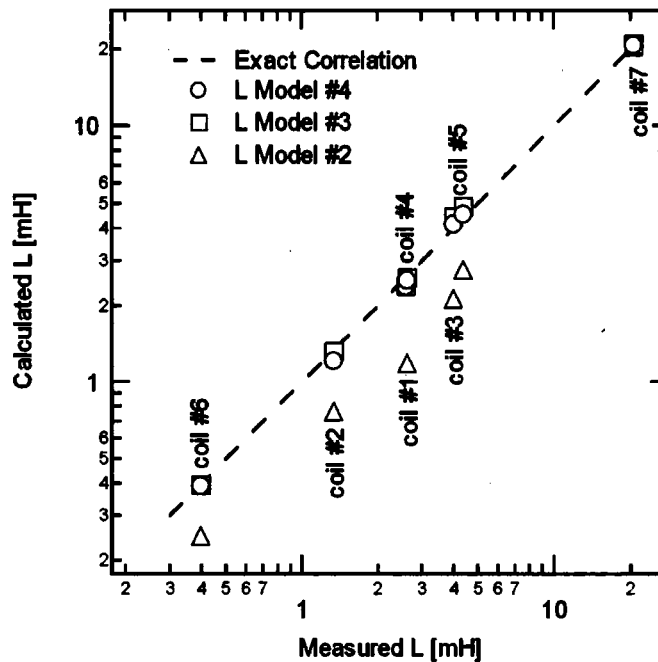

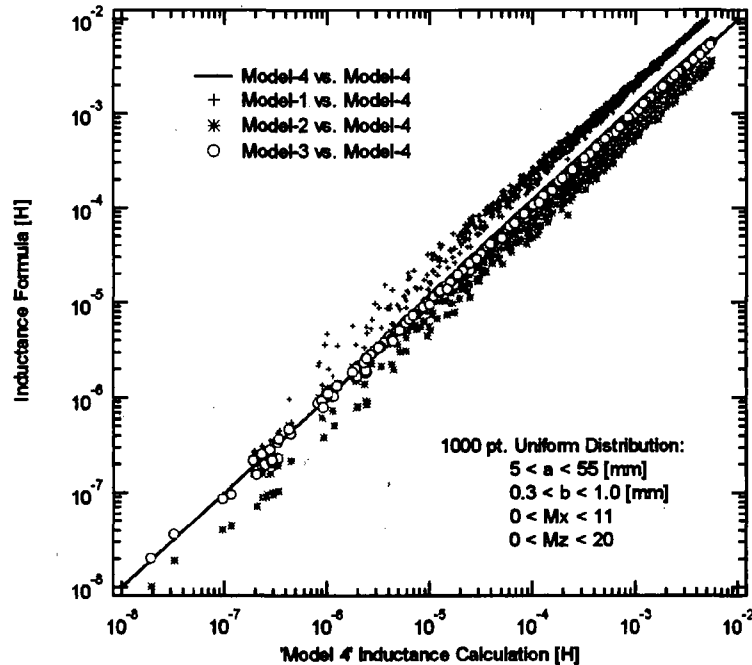Figure 9. Measured vs. calculated inductance.

13

Figure 10. Monte Carlos test of inductance formulas.

Even though these computational methods may seem "brute force" by traditional standards, the computational power of today's desktop computers makes this approach very practical.

References

[1] Jackson, J. D., *Classical Electrodynamics*, 3rd Edition, John Wiley & Sons, 1998, pp. 181–183.

[2] Garrett, Milan Wayne, "Calculation of Fields, Forces, and Mutual Inductances of Current Systems by Elliptic Integrals," *Journal of Applied Physics*, 34(9), September 1963, pp. 2567–2573.

[3] Simpson, James, et al., "Simple Analytic Expressions for the Magnetic Field of a Circular Current Loop," submitted to IEEE *Transactions on Magnetics*, April 1, 2001.

[4] Rosensweig, R. E., *Ferrohydrodynamics*, Dover Publications, Inc., 1985, p. 15.

[5] Whitaker, Jerry C., *The Electronics Handbook*, CRC Press & IEEE Press, 1996, p. 149.

[6] Welsby, V. G., *The Theory and Design of Inductance Coils*, John Wiley & Sons, 1960, p. 44.

APPENDIX A.   COMPONENTS OF MATRIX P

i	p_i
1	$\dfrac{C\,z}{2\alpha^4\beta^3\rho^4}\left[a^4\left(\gamma^2(3z^2-a^2)+\rho^2(8x^2-y^2)\right)\right.$ $-a^2\left(\rho^4(5x^2+y^2)-2\rho^2z^2(2x^2+y^2)+3z^4\gamma^2\right)$ $\left.-R^4\left(2x^4+\gamma^2(y^2+z^2)\right)\right]$
2	$\dfrac{C\,x\,y\,z}{2\alpha^4\beta^3\rho^4}\left[3a^4(3\rho^2-2z^2)-R^4(2R^2+\rho^2)\right.$ $\left.-2a^6-2a^2(2\rho^4-\rho^2z^2+3z^4)\right]$
3	$\dfrac{C\,x}{2\alpha^4\beta^3\rho^2}\left[(\rho^2-a^2)^2(\rho^2+a^2)\right.$ $\left.+2z^2(a^4-6a^2\rho^2+\rho^4)+z^4(a^2+\rho^2)\right]$
4	$\dfrac{C\,z}{2\alpha^4\beta^3\rho^4}\left[a^6\gamma^2+a^4\left(3\gamma^2z^2-\rho^2(x^2-8y^2)\right)\right.$ $+a^2\left(2\rho^2z^2(x^2+2y^2)-\rho^4(x^2+5y^2)+3\gamma^2z^4\right)$ $\left.+R^4\left(\gamma^2(x^2+z^2)-2y^4\right)\right]$
5	$\dfrac{C\,z}{2\alpha^4\beta^3}\left[6a^2(\rho^2-z^2)-7a^4+R^4\right]$

APPENDIX B.   COMPONENTS OF MATRIX Q

j	q_j
1	$\dfrac{C\,z}{2\alpha^4\beta^3\rho^4}\Big[a^2\big(\gamma^2(a^2+2z^2)-\rho^2(3x^2-2y^2)\big)$ $+R^2\big(2x^4+\gamma^2(y^2+z^2)\big)\Big]$
2	$\dfrac{C\,x\,y\,z}{2\alpha^4\beta^3\rho^4}\Big[R^2(2R^2+\rho^2)-a^2(5\rho^2-4z^2)+2a^4\Big]$
3	$-\dfrac{C\,x}{2\alpha^4\beta^3\rho^2}\Big[(\rho^2-a^2)^2+z^2(\rho^2+a^2)\Big]$
4	$-\dfrac{C\,z}{2\alpha^4\beta^3\rho^4}\Big[a^4\gamma^2+a^2\big(2\gamma^2z^2-\rho^2(2x^2-3y^2)\big)+$ $R^2\big(\gamma^2(y^2+z^2)-2y^4\big)\Big]$
5	$\dfrac{C\,z}{2\alpha^4\beta^3}\Big[a^2-R^2\Big]$